Calcium-ion mediated assembly and function of glycosylated flagellar sheath of marine magnetotactic bacterium

Christopher T. Lefèvre, Claire-Lise Santini, Alain Bernadac, Wei-Jia Zhang, Ying Li, Long-Fei Wu

molecular microbiology

Calcium-ion mediated assembly and function of glycosylated flagellar sheath of marine magnetotactic bacterium

Journal:	*Molecular Microbiology*
Manuscript ID:	MMI-2010-10504.R1
Manuscript Type:	Research Article
Date Submitted by the Author:	15-Sep-2010
Complete List of Authors:	Lefèvre, Christopher; CNRS, LCB Santini, Claire-Lise; CNRS, LCB Bernadac, Alain; CNRS, LCB Zhang, Wei-Jia; CNRS, LCB Li, Ying; China Agricultural University, State Key Laboratories for Agro-biotechnology and College of Biological Sciences Wu, Long-Fei; wu@ibsm.cnrs-mrs.fr, CNRS
Key Words:	flagella, Sheath, Calcium ions, Glycoprotein, Magnetotaxis

Calcium-ion mediated assembly and function of glycosylated flagellar sheath of marine magnetotactic bacterium

Christopher T. Lefèvre [1,5,#], Claire-Lise Santini[1,4,#], Alain Bernadac[2,#], Wei-Jia Zhang[1,3,4], Ying Li[3,4] and Long-Fei Wu[1,4]*

[1] Laboratoire de Chimie Bactérienne, UPR9043, Université de la Méditerranée Aix-Marseille II, CNRS, F-13402 Marseille Cedex 20, France

[2] Service de Microscopie Electronique, Institut de Microbiologie de la Méditerranée, CNRS, F13402 Marseille cedex 20, France.

[3] State Key Laboratories for Agro-biotechnology and College of Biological Sciences, China Agricultural University, Beijing 100193, China

[4] Laboratoire International Associé de la Biomineralisation et Nanostructure, CNRS-Marseille, 13402 France.

[5] current address: School of Life Sciences, University of Nevada at Las Vegas, Las Vegas, Nevada 89154-4004, USA

[#] These authors contributed equally to this work

* For correspondence: Long-Fei Wu, LCB IMM CNRS, 31 chemin Joseph Aiguier, F13402 Marseille cedex 20, France. wu@ifr88.cnrs-mrs.fr; phone: 33-4 9115 4157; Fax: 33-4 91718914

Running title: Flagellar sheath of magnetotactic bacteria

24 Key words: flagella/Sheath/Calcium/Glycoprotein/Magnetotaxis

Summary

Flagella of some pathogens or marine microbes are sheathed by an apparent extension of the outer cell membrane. Although flagellar sheath has been reported for almost 60 years, little is known about its function and the mechanism of its assembly. Recently, we have observed a novel type of sheath that encloses a flagellar bundle, instead of a single flagellum, in a marine magnetotactic bacterium MO-1. Here, we reported isolation and characterization of the sheath which can be described as a six-start, right-handed helical tubular structure with a diameter of about 100 nm, and a pitch of helix of about 260 nm. By proteomic, microscopic and immuno-labelling analyses, we showed that the sheath of MO-1 consists of glycoprotein with an apparent molecular mass >350 kDa. This protein, named sheath associated protein (Sap), shows homology with bacterial adhesins and eukaryotic calcium-dependent adherent proteins (cadherin). Most importantly, we showed that calcium ions mediate the assembly of the tubular-shaped sheath and disintegration of the sheath was deleterious for smooth-swimming of MO-1 cells. The disintegrated sheath was efficiently reconstituted in vitro by adding calcium ions. Altogether, these results demonstrate a novel bacterial Ca^{2+}-dependent surface architecture, which is essential for bacterial swimming.

Introduction

Flagella provide bacteria with a highly efficient means of locomotion and also play a central role in adhesion, biofilm formation, and host invasion (McCarter, 2001; Terashima et al., 2008). The flagella are powered by reversible rotary motors embedded in the cell membrane. Beside the function of locomotion they also act as a protein export-assembly apparatus (Macnab, 2003). Tens of thousands copies of a single flagellin protein or of several closely related flagellins are self-assembled to form a hollow concentric double-tubular structures, called simple or complex flagellum, respectively. Flagellins and other exported substrates diffuse down the narrow channel in the growing filament structure and assembly at the distal ends. Recently, it has been shown that glycosylation of flagellins is an important component of numerous flagellar systems in both archaea and bacteria (Logan, 2006). The glycosylation plays either an integral role in assembly or for a number of pathogenic bacteria a role in virulence.

The number and organization of bacterial flagella vary from species to species. The most extensively studied are polar and peritrichous flagella. Interestingly, the polar flagella are surrounded by sheaths in several bacteria including marine *Vibrio* species (Furuno et al., 2000; McCarter, 2001), *Vibrio cholera* (Fuerst and Perry, 1988; Hranitzky et al., 1980), *Bdellovibrio bacteriovorus* (Thomashow and Rittenberg, 1985), *Pseudomonas stizolobii* (Fuerst and Hayward, 1969), *Helicobacter pylori* (Geis et al., 1993; Luke and Penn, 1995; O'Toole et al., 1995), and *Azospirillum brasilense* (Burygin et al., 2007). Each sheath encloses one flagellar filament. How a sheathed flagellum rotates has not been elucidated, and little is known about the composition, formation, or function of flagellar sheaths. Evidence from these organisms suggests that the sheath contains both lipopolysaccharide and proteins with molecular weight ranging from 18 to

61 kDa (Furuno et al., 2000; Hranitzky et al., 1980; Jones et al., 1997). The sheath protein HpaA of *H. pylori* has been localized in the cytoplasm (O'Toole et al., 1995) or on the flagellar sheath (Jones et al., 1997). The mechanism of its secretion and assembly remains unknown. The procedure of sheath formation is suggested to be independent of filament polymerization, since empty flagellar sheaths have been observed as tubule projections originating from the cell surface (Allen and Baumann, 1971). Moreover, the sheath in *Vibrio parahaemolyticus* seems to act on retaining flagellin monomers and allowing subunit assembly (McCarter, 1995). Despite the extensive microscopic and molecular studies, the requirement of the sheath for bacterial motility has not been reported.

Recently, we reported a peculiar architecture of the flagellar apparatus of marine magnetotactic bacteria MO-1 (Lefèvre et al., 2009). Magnetotactic bacteria (MTB) consist of a heterogeneous group of gram negative bacteria that synthesize intracellular crystals of magnetic iron oxide and/or iron sulfide minerals (Bazylinski and Frankel, 2004). These membrane-bounded crystals, called magnetosomes, align forming an intracellular magnetic dipole moment and allow the bacteria to orient and migrate along geomagnetic field lines. This behavior, called magneto-aerotaxis, increases the efficiency of cells to find and maintain at a preferred position at the oxic-anoxic transition zone (OATZ) (Bazylinski and Frankel, 2004). Like most magnetotactic coccoid cells studied, MO-1 cells are bilophotrichously flagellated, having two flagellar bundles on one hemisphere of the cells (Lefèvre et al., 2009). We have reported for the first time that these flagellar bundles are enclosed within sheaths. In this study, we identified the major sheath associated protein (Sap) as a large glycosylated polypeptide. Most importantly, we showed that calcium ions play an essential role in the assembly of tubular-shaped sheath, and that the sheath is required for smooth swimming of MO-1 cells.

Results

Biochemical characterization of MO-1 surface appendages

To investigate their biochemical composition, surface appendages of MO-1 were detached from cell by shearing and centrifugation. The final fractions named C2 contained flagella, sheaths and membrane vesicles as revealed by transmission electron microscopy (TEM) analysis (Fig. 1A). In the C2 fraction, sheaths were separated from the flagella, indicating a loose connection between the internal core of flagella bundle and external sheath. Although detached from the flagella bundle, the sheath remained as nanotube, but broken into shorter fragments due to the shearing. Image analysis suggests that the sheath can be described as a six-start (composed of six protofilaments), right-handed helical tubular structure with a diameter of about 100 nm, and a pitch of helix of about 260 nm (Fig. 1, panels C to E).

The protein composition of the C2 fraction was analyzed by SDS-PAGE and Coomassie Blue staining. The C2 fraction was apparently composed of 7 polypeptide bands (IN and M1 to M6, Fig. 1F, lane 2). IN was located in the stacking gel and not further studied. Periodic acid Schiff staining showed that M1, M2, M5 and M6 were glycoproteins (Fig. 1F, lane 2s). In addition, Azur blue staining revealed a polyanionic nature of the glycans on these polypeptides (Supporting Information, Fig. S1). N-terminal sequencing and ion-trap MS-MS mass spectroscopy analyses revealed that the polypeptides M4, M5 and M6 were homologous to flagellin proteins from various bacteria, including the closely related *Candidatus* Magnetococcus marinus strain MC-1 (Schubbe et al., 2009). Intriguingly, MC-1 genome contains 15 flagellin encoding genes and the predicted flagellins exhibit similar molecular sizes and pI values (Schubbe et al., 2009). It is likely that the genome of MO-1 contains multiple copies of flagellins. Recently, it has been reported that inactivation of the flagellin gene *flaA* in

Magnetospirillum gryphiswaldense results in nonmagnetotactic mutants lacking flagellar filaments (Schultheiss *et al.*, 2004). The N-terminus of the polypeptide M3 was homologous to the hypothetical protein Mmc1_3749 of *Cand.* M. marinus MC-1 (Schubbe et al., 2009). The N-terminal sequence of M2 (PTITASNLT) did not possess 100% sequence identity with any protein in the NCBI database. The identity of this polypeptide remains to be determined.

The polypeptide M1 particularly drew our attention. Autolysis of C2 fractions at 37 °C for 4 days led to the concomitant disappearance of M1 polypeptide and the sheaths (Fig. 1B, Fig. 1F, lane 3 compared to lane 2), whereas the other five polypeptides and flagella and vesicles remained intact. To further analyze the relationship between the M1 protein and the sheath structure, we excised the polypeptide band of M1 and used it to raise polyclonal antibodies. Immunoblot analyses confirmed the specificity of the polyclonal antibody obtained; only M1 was detected in the crude extracts or the C2 fractions of MO-1 by this antiserum (Fig. 2, inset panel). Using anti-M1 antibody-based immuno-gold staining, we found that the gold-particles specifically localized on the sheath (Fig. 2). These results strongly suggest that the M1 protein is a component of the sheath.

To identify the M1 polypeptide, protein samples in the M1 band were digested with trypsin and then analyzed by Microflex MALDI-ToF, ESI-Q-ToF and nLC-ESI-MS/MS mass spectrometry. Searching in the MO-1 genomic contig database unambiguously identified M1 as product of a gene encompassing 10068 bp (accession HM015774) and encoding 3356 amino acids with a predicated molecular weight of 344502.6 Da and a pI of 3.29 (see Supporting Information, Fig S2). In addition, the N-terminal sequence (AATPTATD) of M1 perfectly matched with the residues 226 to 233 of the gene product, suggesting a posttranslational processing of the precursor. We designate the gene as *sap* for its product sheath-associated protein.

BlastP searching in NCBI database revealed that Sap is homologous primarily with outer membrane adhesin like proteins from various bacteria, and the most closely related is that from *Cand*. M. marinus strain MC-1 (42% identity with putative outer membrane adhesin like protein, accession YP_865069.1). COGnitor analysis showed that Sap contains three segments belonging to the cluster of orthologous group of large exoproteins involved in heme utilization or adhesion (COG3210) and three segments belonging to COG5292 (autotransporter adhesion). InterProScan analysis showed that C-terminus of Sap possesses one Cadherin_2 domain (IPR002126, at position 2257-2331) and one Cadherin-like domain (IPR015919, at position 2441-2535). Cadherins represent a major superfamily of transmembrane glycoproteins that mediate calcium-dependent cell-cell adhesion in both vertebrates and invertebrates (Takeichi, 1991). Canonical cadherins have an extracellular domain in the N-terminal part of the molecule, which typically is composed of five cadherin repeats. Proteins are designated as members of the broadly defined cadherin family if they have one or more cadherin repeats. As it contains 2 predicated cadherin repeats, Sap can be considered as a novel member of the cadherin family.

Calcium-ions are crucial for the sheath structure

As implied in the name, cadherins (for calcium-dependent adherent proteins) require calcium ions for assembly of protein domains and subunit into highly organized functional structures. Calcium ions bind to specific residues (Asp, Asn, Glu and Gln) in cadherin repeats to ensure its proper folding and to confer rigidity upon the extracellular domain. Therefore, calcium ions are essential for cadherin adhesive function and for protection against protease digestion (Takeichi, 1991). The Sap protein of MO-1 contains cadherin-repeat-domains and is rich in residues Asp (12.7%), Asn (5.8%) and Glu (5.2%). Hence, we sought to assess the involvement of calcium ions in establishing the structure of the sheaths.

The solutions used in C2 fractions preparation appeared to be important for the sheath structure. The synthetic seawater seemed to have beneficial effect on the stability of the sheath. Addition of divalent ion chelators led to the disappearance of the sheaths from the C2 fractions, whereas the flagella and vesicles remained intact (Fig. 3A). Interestingly, the chelate treatment did not modify protein patterns of the C2 fractions on SDS-PAGE gels (data not shown). These results suggest that chelators disintegrate the structure of the sheaths, implying a crucial role of calcium ions for the structure.

To corroborate this hypothesis, we assessed the possibility to reconstitute the sheaths from disintegrated components. The citrate-treated sheath-free C2 fractions were incubated with addition of $CaCl_2$ or $MgCl_2$, or both. As shown in Fig. 3, only calcium ions allowed reconstitution of the sheath structure. The same results were obtained when the sheaths were disintegrated with EGTA (ethylene glycol tetraacetic acid chelating specifically calcium ions) (see Supporting Information, Fig S3) or EDTA (ethylene diamine tetraacetic acid). Therefore, calcium ions seem to specifically mediate the reconstitution of the sheath structure.

Requirement of the flagellar sheath for the smooth swimming of MO-1 cells

Although it has been over sixty years since the first report of flagellar sheath, its function in bacterial motility remain undemonstrated. The disintegration of the flagellar sheath by citrate provides an effective means to analyze sheath function. Figure 4 shows a typical TEM image of MO-1 cell after treatment with sodium citrate, flagella are dispersed resulting from disintegration of sheath (Fig. 4A2 versus 4A1). The extent of disintegration augmented with increased concentration of citrate and prolonged incubation time. The impact of citrate treatment on cell motility was analyzed using dark field optical microscopy. Typically, MO-1 cells exhibit two patterns of motility; forward smooth-swimming and circumgyrating. Whereas smooth-swimming

bacteria exhibited a helical trajectory (Fig. 4B, 's' symbol), circumgyrating cells appeared as bright spots, or rosette (Fig. 4B, 'c' symbols and inset) when observed at high amplification. The circumgyrating swimming might result from either disordered flagellar rotation or adhesion of flagella to the slides. Non motile bacteria also appeared as spots, generally sharper and smaller than the circumgyrating cells (Fig. 4B). We quantified the helical trajectories and the spots using Image J software. Without citrate treatment, about half of MO-1 cells (43.3±7.9%, average ± standard deviation, n=618 cells analyzed) swam smoothly with swimming velocity of 126 ± 10 µm s^{-1}. The percentage and the velocity of smooth swimming bacteria decreased in direct proportion with the increase of citrate concentration (Fig. 4C1 and 4C2, respectively). When sodium citrate was added at 50 mM, less than 1% cells swam smoothly with velocity of 49 ± 11 µm s^{-1} (n=312). Moreover, addition of magnesium or calcium ions relieved the deleterious effect of citrate on bacterial motility (Fig. 4D). Under these conditions, the sheath structure remained intact. Statistic analysis confirms that harmful effect of citrate on the smooth swimming is significant compared to the untreated cells or cells protected by divalent ions (Table 1). Together these results reveal that the sheath of the flagellar bundle is crucial for the smooth swimming of MO-1 cells.

Discussion

Since the first observation in *Vibrio metchnikovii* in 1947 (Van Iterson, 1947), single flagellar sheath that cover only one polar flagellum has been reported for several bacterial species. Microscopic studies together with immunolabeling analyses revealed that the single flagellum sheath is a continuation of the cell wall (Burygin et al., 2007; Fuerst and Perry, 1988; Glauert, 1968). Interestingly, Hranitzky et al. have reported that although the sheath protein was detected

on the flagellum as well as on the outer membrane of the *V. cholera* cells, antibody specific for lipopolysaccharide labeled the cell but not the sheathed flagellum (Hranitzky et al., 1980). Therefore, they proposed that the sheath is not a simple extension of the outer membrane. In this study, immuno-fluorescence analysis revealed that Sap also locate on the surface of the MO-1 cells (Supporting information, Fig S4). However, immune-gold labeled only sheath disconnected from the cells or the isolated sheath, but not the cell surface (data not shown). The discrepancy of the results might be due to the difference between the two immune-detection procedures used. Fluorescein is a small molecule with a mass of about 332 Dalton (<1 nm). In contrast the gold particle has a big size of about 7 nm. Therefore, fluorescein marker has a better accessibility than gold particles. In addition, MO-1 cells are rich in phosphor and lipid granules, which considerably reduced the contrast between cells and the gold particles and made the observation difficult. It is unknown how the Sap protein is secreted to the cellular surface and how they assemble at precise position to form the sheath. N-terminal sequencing revealed that the first 225 residues are absent from the mature Sap, implying a processing of the precursor during Sap secretion. As the potentially processed segment does not carry any known protein targeting signal sequence, a novel protein targeting and secretion mechanism might be involved in sheath assembly.

Calcium ions impact nearly every aspect of cellular life. Ca^{2+}-binding triggers changes in protein shape and charge, participates in a variety of cellular processes in both eukaryotic and prokaryotic organisms (Clapham, 2007; Dominguez, 2004). Eukaryotic extracellular matrix hosts a large variety of Ca^{2+}-binding proteins (Maurer et al., 1996). For example, human fibrillin-1 is a 350 kDa calcium binding glycoprotein, which assembles to form 10-12 nm microfibrils in extracellular matrix (Handford, 2000). MO-1 Sap protein shares similarity with fibrillin-1 in that

both are exported large glycoproteins and assemble into higher order structures in a calcium ion-dependent manner. To our knowledge, the MO-1 sheath is the only known bacterial extracellular calcium dependent architecture assembled from glycoprotein. Sequence similarity between Sap and cadherins would suggest that calcium ions bind to residues Asp, Asn, Glu and Gln rather than directly to glycans of Sap as that occurs in cadherins. Autolysis or treatment of flagella with hydrochloric acid or urea resulted in loss of the sheaths of *V. metchnikovii* and *P. stizolobii* flagella (Follett and Gordon, 1963; Fuerst and Hayward, 1969), implying a fragile structure of the single flagellum sheath. Here we showed that removing calcium ions by chelators disintegrates the MO-1 sheaths. It is unknown whether the assembly of the single flagellum sheath is mediated by the calcium ions and if the same mechanism is involved in the assembly of both single flagellum and multiple flagella sheath.

Once thought to be restricted to eukaryotes, glycosylation is now being increasingly reported in prokaryotes (Spiro, 2002). Examples of bacterial glycoproteins include, among others, the flagellins of *Pseudomonas aeruginosa* (Takeuchi et al., 2003) and *Campylobacter* spp. (Doig et al., 1996), the type IV pili of *P. aeruginosa* (Castric, 1995) and *Neisseria meningitides* (Power et al., 2003), the Fap1 fimbrial adhesin of *Streptococcus parasanguinis* (Stephenson et al., 2002), the high-molecular-weight protein (HmwA) of *Haemophilus influenzae* (Grass et al., 2003), and the autotransporter protein Ag43 of *Escherichia coli* (Sherlock et al., 2006). It is evident that glycosylation plays a vital role in pathogenicity and host invasion (Szymanski and Wren, 2005). Interestingly, impairment of flagellin glycosylation in *Pseudomonas syringae* pv. tabaci decreases bacterial swimming activity in a highly viscous medium and affects polymorphic transitions and the bundle formation of peritrichous flagella (Taguchi et al., 2008). It has been proposed that glycosylation stabilizes the filament structure and lubricates the rotation of the

bundle. Lubricant function of glycoproteins in human body has been demonstrate (Hills, 2000). In this study we found that both the major sheath protein Sap and flagellins are glycosylated. Considering that seven flagella rotate within the sheath, probably at very high frequency, it seems reasonable to propose that, apart from other functions, the glycans on the sheath and flagella of MO-1 cells might serve as lubricants to reduce the mechanical friction. At present, we don't know if the same system is involved in the glycosylation of the flagellin and the sheath proteins. In addition, whether the glycosylation is essential for the export, assembly and/or function of sheath and flagellins remains an open question.

Little is known about the function of the bacterial flagellar sheath. It has been suggested that the sheath may serve as a protective covering since sheathed polar flagella appear to be more resistant to protease hydrolysis and mechanical treatment than unsheathed peritrichous flagella do. In addition, flagellum sheaths of *V. cholerae* and *H. pylori* have been proposed to serve as a carrier of adhesins (Evans et al., 1993; Fuerst and Perry, 1988), being important for specific interactions with the environment. However, the functional significance of the sheath in bacterial motility is unknown. The feature of the Ca^{2+}-dependent assembly of MO-1 flagellar sheath allowed us to address this question. Disintegration of the sheath apparently has a deleterious effect on the smooth swimming of the MO-1 cells. It is expectable that rotation of seven individual flagella at high frequency within a bundle must be mechanically and structurally coordinated. We have observed the same sheath structure in uncultivated coccoid-ovoid Mediterranean magnetotactic bacteria collected at Ile des Embiez (Lefèvre et al., 2009). In addition, the *Cand*. M. marinus MC-1 strain isolated from the Pettaquamscutt Estuary in USA (D. A. Bazylinski, personal communication), an axenic magnetotactic coccus culture isolated from a hypersaline sea, the Salton Sea, California (C. T. Lefèvre, and D. A. Bazylinski,

unpublished), uncultivated magnetotactic cocci collected from the China Sea (Zhou et al., 2010) and Mediterranean Sea (N. Pradel, personal communication) seem to contain the same bilophotrichous flagella and sheath structure as the MO-1 cells. Evolution might have selected the Ca^{2+}-mediated sheath structure to ensure harmonious rotation of the flagella within the bundles to achieve an efficient magneto-aerotaxis of marine cocci. Elucidation of the mechanism of flagellar sheath synthesis challenges current knowledge of secretion and assembly of glycoproteins into the remarkable extracellular locomotion apparatus.

Experimental procedures

Extraction and analysis of the flagellar apparatus

Magneto-ovoid strain MO-1 was incubated in the EMS2 medium at 24°C to exponential phase (Lefèvre et al., 2009). Cells were collected by centrifugation at 14 000 g for 10 min, resuspended with synthetic seawater (332 mM NaCl, 29 mM $MgCl_2$, 23 mM Na_2SO_4, 16 mM $CaCl_2$, 7 mM KCl in 12.5 mM pH7.2 HEPES buffer), and cell suspension was pushed through syringe needles (0.8x40 mm) 20 times to shear the flagellar propellers. Sheared cells were centrifuged at 20 000 g for 5 min to separate cells and cellular debris from the flagellar propellers. The supernatants were further centrifuged at 200 000 g for 50 min, and the pellets (C2) were resuspended with the synthetic seawater if not mentioned specially. In general, protein samples are maintained at low temperature (on ice or at 4°C) to prevent the proteolysis. Autolysis of C2 fraction was thus performed by incubating at 37°C for 4 days. Analysis of microscopes and SDS-PAGE were made as previously described (Pradel et al., 2006).

Glycosylated proteins were visualized by Periodic acid-Schiff staining according to Zacharius *et al.* (Zacharius et al., 1969).

To study the disintegration of the sheath, the pellets C2 were resuspended with synthetic seawater or HEPES buffer (12.5 mM, pH=7.2), supplemented with generally used calcium chelator such as EDTA, EGTA or sodium citrate at the final concentrations as indicated in the text. After incubation in ice for 45 min, C2 fractions were ultracentrifuged and the pellets were resuspended with modified synthetic seawater without divalent ions, or supplemented with 16 mM $CaCl_2$ or 29 mM $MgCl_2$, or both and incubated at room temperature for 45 min. The presence of sheath was examined under electron microscope.

Measurement of swimming velocities

MO-1 cells at exponential growth phase were collected and distributed into microtubes. HEPES buffer (25 mM, pH 7.2 supplemented with 328 mM NaCl, 22.8 mM Na_2SO_4, and 7.4 mM KCl) was added at 1/10 volume to the cell suspensions. When required, sodium citrate (at final concentrations as indicated in text), $CaCl_2$ (added at 1/10 volume from supernatant of saturated solution in the HEPES buffer), or $MgCl_2$ (50 mM in the HEPES buffer) were added at time zero. After one to six hours of treatment, seven microliter aliquots of cell suspensions were dropped onto microscope slides and covered with 22 x 22 mm cover slips, and observed using a 40x objective on a ZEISS Photomicroscope III microscope under dark field. Swimming tracks were recorded with a Photonic Scientific CCD camera controlled by Image-Pro program with exposure time of 100 ms, and the images were analyzed using Image J. Statistics were done with Origin 8 software.

Electron microscopy

Transmission electron microscopic analysis was as described previously (Pradel et al., 2006). Image-Pro plus was used for inverse Fourier transform analysis of the TEM images. For image enhancement the major peaks in the Fourier Transform were amplified. Polypeptides M1 were

318 excised from the polyacrylamid gels and used to generate rabbit polyclonal antibodies by using
319 conventional protocol (Harlow and Lane, 1988). Immuno-gold staining using polyclonal rabbit
320 anti-M1 at dilution of 1/1500 and 7 nm gold-conjugated protein A was performed as described
321 by Pradel et al. (Pradel et al., 2006).
322
323 **Acknowledgment**
324 We thank N. Philippe and C. Nicoletti for helpful discussion and suggestion, S. Lignon and R.
325 Lebrun for proteomic analysis. This work was supported by the grants HFSP RGP0035/2004-C,
326 FRM FDT20080913879 and 'The Project for Extramural Scientists of SKLAB No.
327 2009SKLAB06-1'.
328
329 **References**
330 Allen, R.D., and Baumann, P. (1971) Structure and arrangement of flagella in species of the
331 genus *Beneckea* and *Photobacterium* fischeri. *J. Bacteriol.* **107**: 295-302.
332 Bazylinski, D.A., and Frankel, R.B. (2004) Magnetosome formation in prokaryotes. *Nat. Rev.*
333 *Microbiol.* **2**: 217-230.
334 Burygin, G., Shirokov, A., Shelud'ko, A., Katsy, E., Shchygolev, S., and Matora, L. (2007)
335 Detection of a sheath on *Azospirillum brasilense* polar flagellum. *Microbiology* **76**: 728-
336 734.
337 Castric, P. (1995) *pilO*, a gene required for glycosylation of *Pseudomonas aeruginosa* 1244
338 pilin. *Microbiology* **141**: 1247-1254.
339 Clapham, D.E. (2007) Calcium signaling. *Cell* **131**: 1047-1058.

340 Doig, P., Kinsella, N., Guerry, P., and Trust, T.J. (1996) Characterization of a post-translational
341 modification of *Campylobacter flagellin*: identification of a sero-specific glycosyl
342 moiety. *Mol. Microbiol.* **19**: 379-387.
343 Dominguez, D.C. (2004) Calcium signalling in bacteria. *Mol Microbiol* **54**: 291-297.
344 Evans, D.G., Karjalainen, T.K., Evans, D.J., Jr., Graham, D.Y., and Lee, C.H. (1993) Cloning,
345 nucleotide sequence, and expression of a gene encoding an adhesin subunit protein of
346 *Helicobacter pylori*. *J. Bacteriol.* **175**: 674-683.
347 Follett, E.A., and Gordon, J. (1963) An electron microscope study of *Vibrio* flagella. *J Gen*
348 *Microbiol* **32**: 235-239.
349 Fuerst, J.A., and Hayward, A.C. (1969) The sheathed flagellum of *Pseudomonas stizolobii*. *J.*
350 *Gen. Microbiol.* **58**: 239-245.
351 Fuerst, J.A., and Perry, J.W. (1988) Demonstration of lipopolysaccharide on sheathed flagella of
352 *Vibrio cholerae* O:1 by protein A-gold immunoelectron microscopy. *J Bacteriol* **170**:
353 1488-1494.
354 Furuno, M., Sato, K., Kawagishi, I., and Homma, M. (2000) Characterization of a flagellar
355 sheath component, PF60, and its structural gene in marine *Vibrio*. *J Biochem* **127**: 29-36.
356 Geis, G., Suerbaum, S., Forsthoff, B., Leying, H., and Opferkuch, W. (1993) Ultrastructure and
357 biochemical studies of the flagellar sheath of *Helicobacter pylori*. *J Med Microbiol* **38**:
358 371-377.
359 Glauert, A.M. (1968) Electron microscopy of lipids and membranes. *J. R. Microsc. Soc.* **88**: 49-
360 70.
361 Grass, S., Buscher, A.Z., Swords, W.E., Apicella, M.A., Barenkamp, S.J., Ozchlewski, N., and
362 III, J.W.S.G. (2003) The *Haemophilus influenza* HMW1 adhesin is glycosylated in a

process that requires HMW1C and phosphoglucomutase, an enzyme involved in lipooligosaccharide biosynthesis. *Mol. Microbiol.* **48**: 737-751.

Handford, P.A. (2000) Fibrillin-1, a calcium binding protein of extracellular matrix. *Biochim Biophys Acta* **1498**: 84-90.

Harlow, E., and Lane, D. (1988) *Antibodies: A laboratory manual.* Cold Spring Harbor, NY: Cold Spring Harbor Laboratory.

Hills, B.A. (2000) Boundary lubrication in vivo. *Proc Inst Mech Eng [H]* **214**: 83-94.

Hranitzky, K.W., Mulholland, A., Larson, A.D., Eubanks, E.R., and Hart, L.T. (1980) Characterization of a flagellar sheath protein of *Vibrio cholerae*. *Infect Immun* **27**: 597-603.

Jones, A.C., Logan, R.P., Foynes, S., Cockayne, A., Wren, B.W., and Penn, C.W. (1997) A flagellar sheath protein of *Helicobacter pylori* is identical to HpaA, a putative N-acetylneuraminyllactose-binding hemagglutinin, but is not an adhesin for AGS cells. *J. Bacteriol.* **179**: 5643-5647.

Lefèvre, C.T., Bernadac, A., Yu-Zhang, K., Pradel, N., and Wu, L.-F. (2009) Isolation and characterization of a magnetotactic bacterial culture from the Mediterranean Sea. *Environ. Microbiol.* **11**: 1646–1657.

Logan, S.M. (2006) Flagellar glycosylation - a new component of the motility repertoire? *Microbiology* **152**: 1249-1262.

Luke, C.J., and Penn, C.W. (1995) Identification of a 29 kDa flagellar sheath protein in Helicobacter pylori using a murine monoclonal antibody. *Microbiol.* **141**: 597-604.

Macnab, R.M. (2003) How bacteria assemble flagella. *Annu. Rev. Microbiol.* **57**: 77-100.

385 Maurer, P., Hohenester, E., and Engel, J. (1996) Extracellular calcium-binding proteins. *Curr.*
386 *Opin. Cell Biol.* **8**: 609-617.
387 McCarter, L.L. (1995) Genetic and molecular characterization of the polar flagellum of *Vibrio*
388 *parahaemolyticus*. *J. Bacteriol.* **177**: 1595-1609.
389 McCarter, L.L. (2001) Polar flagellar motility of the Vibrionaceae. *Microbiol. Mol. Biol. Rev.*
390 **65**: 445-462.
391 O'Toole, P.W., Janzon, L., Doig, P., Huang, J., Kostrzynska, M., and Trust, T.J. (1995) The
392 putative neuraminyllactose-binding hemagglutinin HpaA of *Helicobacter pylori* CCUG
393 17874 is a lipoprotein. *J. Bacteriol.* **177**: 6049-6057.
394 Power, P.M., Roddam, L.F., Rutter, K., Fitzpatrick, S.Z., Srikhanta, Y.N., and Jennings, M.P.
395 (2003) Genetic characterization of pilin glycosylation and phase variation in *Neisseria*
396 *meningitidis*. *Mol. Microbiol.* **49**: 833-837.
397 Pradel, N., Santini, C.L., Bernadac, A., Fukumori, Y., and Wu, L.-F. (2006) Biogenesis of actin-
398 like bacterial cytoskeletal filaments destined for positioning prokaryotic magnetic
399 organelles. *Proc. Natl. Acad. Sci. USA* **103**: 17485-17489.
400 Schubbe, S., Williams, T.J., Xie, G., Kiss, H.E., Brettin, T.S., Martinez, D., Ross, C.A., Schuler,
401 D., Cox, B.L., Nealson, K.H., and Bazylinski, D.A. (2009) Complete genome sequence
402 of the chemolithoautotrophic marine magnetotactic coccus strain MC-1. *Appl Environ*
403 *Microbiol* **75**: 4835-4852.
404 Schultheiss, D., Kube, M., and Schuler, D. (2004) Inactivation of the flagellin gene *flaA* in
405 *Magnetospirillum gryphiswaldense* results in nonmagnetotactic mutants lacking flagellar
406 filaments. *Appl Environ Microbiol* **70**: 3624-3631.

Sherlock, O., Dobrindt, U., Jensen, J.B., Vejborg, R.M., and Klemm, P. (2006) Glycosylation of the self-recognizing *Escherichia coli* Ag43 autotransporter protein. *J. Bacteriol.* **188**: 1798-1807.

Spiro, R.G. (2002) Protein glycosylation: nature, distribution, enzymatic formation, and disease implications of glycopeptide bonds. *Glycobiol.* **12**: 43R-56R.

Stephenson, A.E., Wu, H., Novak, J., Tomana, M., Mintz, K., and Fives-Taylor, P. (2002) The Fap1 fimbrial adhesin is a glycoprotein: antibodies specific for the glycan moiety block the adhesion of *Streptococcus parasanguis* in an in vitro tooth model. *Mol. Microbiol.* **43**: 147-157.

Szymanski, C.M., and Wren, B.W. (2005) Protein glycosylation in bacterial mucosal pathogens. *Nat. Rev. Microbiol.* **3**: 225-237.

Taguchi, F., Shibata, S., Suzuki, T., Ogawa, Y., Aizawa, S., Takeuchi, K., and Ichinose, Y. (2008) Effects of glycosylation on swimming ability and flagellar polymorphic transformation in *Pseudomonas syringae* pv. tabaci 6605. *J. Bacteriol.* **190**: 764-768.

Takeichi, M. (1991) Cadherin cell adhesion receptors as a morphogenetic regulator. *Science* **251**: 1451-1455.

Takeuchi, K., Taguchi, F., Inagaki, Y., Toyoda, K., Shiraishi, T., and Ichinose, Y. (2003) Flagellin glycosylation island in *Pseudomonas syringae* pv. *glycinea* and its role in host specificity. *J. Bacteriol.* **185**: 6658-6665.

Terashima, H., Kojima, S., and Homma, M. (2008) Flagellar motility in bacteria structure and function of flagellar motor. *Int Rev Cell Mol Biol* **270**: 39-85.

Thomashow, L.S., and Rittenberg, S.C. (1985) Isolation and composition of sheathed flagella from *Bdellovibrio bacteriovorus* 109J. *J. Bacteriol.* **163**: 1047-1054.

Van Iterson, W. (1947) Some electron-microscopical observations on bacterial cytology. *Biochim. Biophys. Acta* **1**: 527-548.

Zacharius, R.M., Zell, T.E., Morrison, J.H., and Woodlock, J.J. (1969) Glycoprotein staining following electrophoresis on acrylamide gels. *Anal. Biochem.* **30**: 148-152.

Zhou, K., Pan, H., Yue, H., Xiao, T., and Wu, L.-F. (2010) Architecture of flagellar apparatus of marine magnetotactic cocci from Qingdao. *Marine Sciences (Chinese)* **Accepted**.

438 Table 1. Significance of the effect of citrate treatment on smooth swimming of MO-1 cells.

439

Treatment[1]	Percentage of mobile cells	Average speed (μm/s)	P value[2]
HEPES buffer	(27.3±7.3) %	114±13	3.8891E-11
HEPES buffer+Citrate	(7.1±5.5)%	72±16	-
HEPES buffer+Citrate+Mg^{2+}	(25.7±10.8)%	108±13	1.7231E-9
HEPES buffer+Citrate+Ca^{2+}	(25.6±7.0)%	100±12	1.3825E-8

440

441

442 1. Composition of the HEPES buffer and concentration of ions used are described in text.

443 2. Two sample t-test of average speed was analyzed by OriginPro 8 software. Each sample was

444 compared with HEPES buffer+Citrate.

445

446

447 **Figure Legends**

448 Figure 1. Composition of extracted surface appendages of MO-1 cells .

449 Intact (A) or autolyzed (B) C2 fractions were inspected under electron microscope. Panels (C),
450 (D) and (E) show original TEM micrograph of a isolated sheath, the amplitude spectrum of
451 Fourier transform, and inverse Fourier transform image after filtering, respectively. Black
452 arrows, black arrow heads and white arrow heads indicate sheaths, flagella and vesicles,
453 respectively. Scale bars show 100 nm. Panel (F): whole cell (lane 1), untreated (lane 2) or
454 autolyzed (lane 3) C2-fractions were resolved on 7.5% polyacrylamide gels by SDS-PAGE and
455 stained by Coomassie blue (lanes 1 to 3,) or Periodic Acid Schiff staining (lane 1s to 3s).
456 Molecular masses (lane M) are indicated as kDa on left.

457

458 Figure 2. Localization of M1 protein. Specificity of polyclonal anti-M1 antibodies was
459 confirmed by recognization of M1 polypeptides in whole cell extracts (inset image, lane 1) or C2
460 fractions (lane 2) by immunoblotting analysis. Molecular masses are indicated as kDa on right.
461 Localization of M1 polypeptides in C2 fractions is revealed by immuno-gold staining by using
462 the polyclonal anti-M1 antibodies. Inset is amplification of the area as indicated by the dashed
463 lines. Black arrow, black arrow head and white arrows indicate sheath, flagellum and gold
464 particles, respectively.

465

466 Figure 3. Reconstitution of the sheath structure.

467 To disintegrate sheaths, C2 fractions were incubated with 50 mM sodium citrate in synthetic
468 seawater in ice for 45 min and centrifuged (see Experimental procedures). The pellets were

resuspended with synthetic seawater without calcium and magnesium (A), or supplemented with $CaCl_2$ and $MgCl_2$ (B), $CaCl_2$ (C) or $MgCl_2$ (D), incubated for 45 min and inspected under TEM. Black arrows, black arrow heads and white arrow heads indicate sheaths, flagella and vesicles, respectively. Scale bars show 100 nm.

Figure 4

Requirement of the sheath for smooth swimming of MO-1 cells.

TEM micrographs show typical untreated (panel A1) or citrate (25 mM) treated MO-1 cells (panel A2). Swimming tracks of MO-1 cells were recorded by using dark field optical microscopy with 100 ms exposure time (panel B), showing the smooth swimming (s) or circumgyrating cells (c). Bars show 0.5 µm in (A1) and (A2), 3 µm in (B) and 1 µm in the inset of (B). Panels C1 and C2 show the effect of increasing concentration of sodium citrate on the proportion of smooth swimming or the velocity of smooth swimming cells, respectively. Panels D1 and D2 show the effect of treatment with sodium citrate without or with magnesium or calcium ions on the proportion of smooth swimming or the velocity of smooth swimming cells, respectively. The values are average plus standard deviation obtained by analysis of more than 10 microscope records.

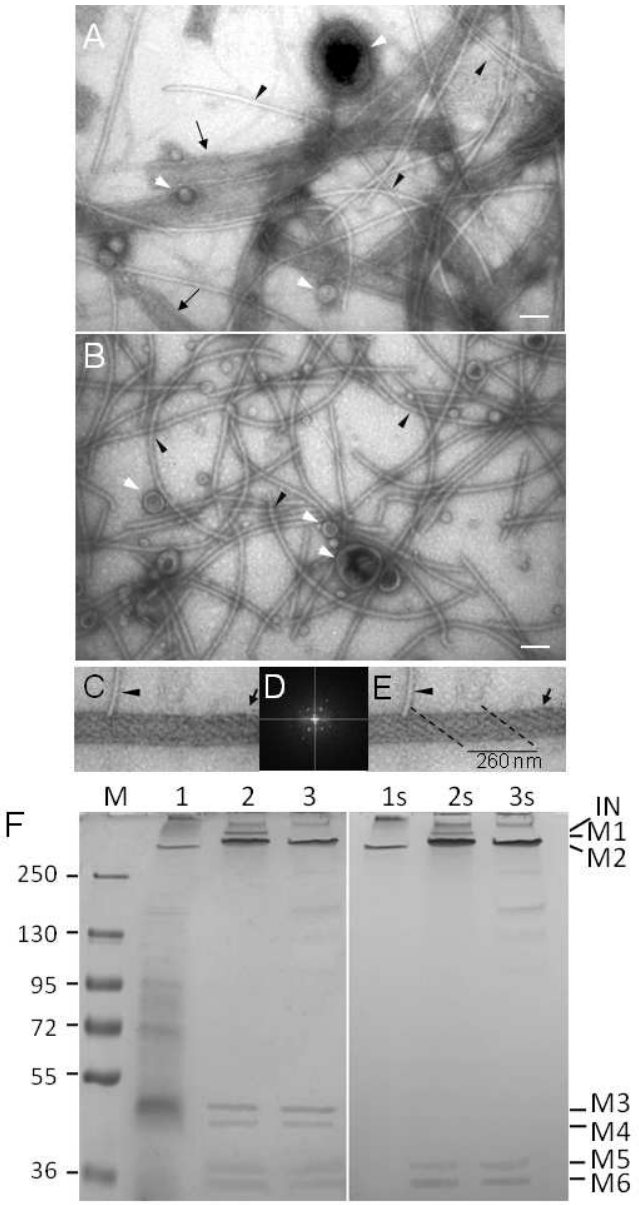

190x254mm (96 x 96 DPI)

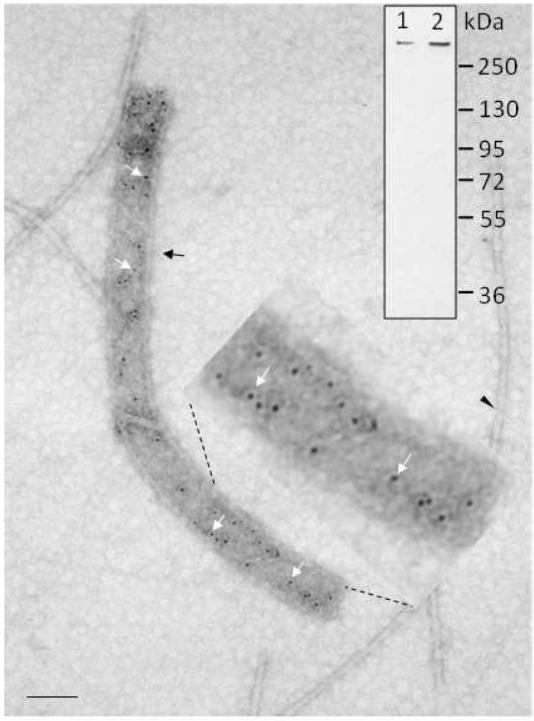

190x254mm (96 x 96 DPI)

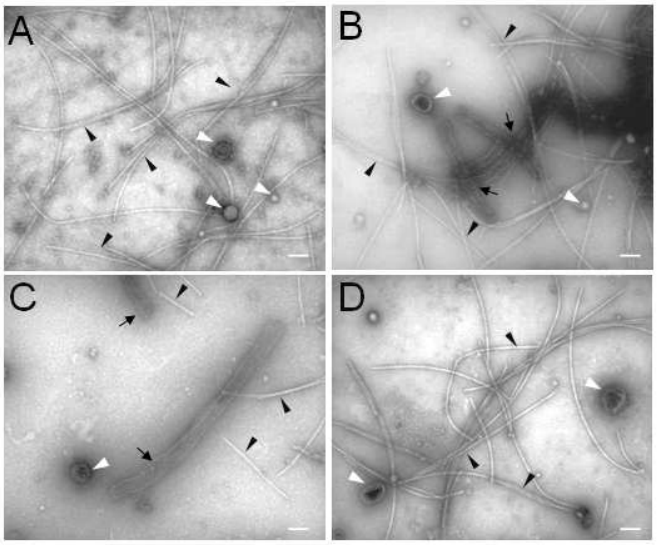

190x254mm (96 x 96 DPI)

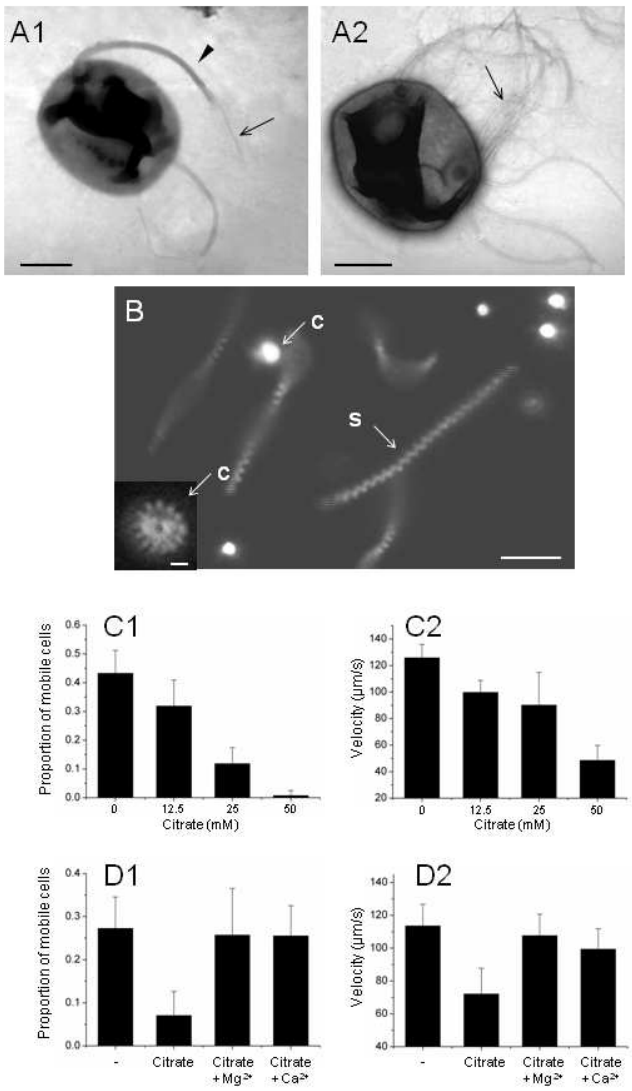

190x254mm (96 x 96 DPI)